

# We are IntechOpen, the world's leading publisher of Open Access books Built by scientists, for scientists

6,900

Open access books available

186,000

International authors and editors

200M

Downloads

Our authors are among the

154

Countries delivered to

TOP 1%

most cited scientists

12.2%

Contributors from top 500 universities



WEB OF SCIENCE™

Selection of our books indexed in the Book Citation Index  
in Web of Science™ Core Collection (BKCI)

Interested in publishing with us?  
Contact [book.department@intechopen.com](mailto:book.department@intechopen.com)

Numbers displayed above are based on latest data collected.  
For more information visit [www.intechopen.com](http://www.intechopen.com)



# Simulation Model of Fragmentation Risk

*Mirko Djelosevic and Goran Tepic*

## Abstract

In this chapter, a simulation model for fragmentation risk assessment due to a cylindrical tank explosion is presented. The proposed fragmentation methodology is based on the application of Monte Carlo simulation and probabilistic mass method. The probabilities of generating fragments during the explosion of the tank were estimated regardless of the available accident data. Aleatoric and epistemic uncertainty due to tank fragmentation has been identified. Generating only one fragment is accompanied by aleatoric uncertainty. The maximum fragmentation probability corresponds to the generation of two fragments with a total mass between 1200 kg and 2400 kg and is 17%. The fragment shape was assessed on the basis of these data and fracture lines. Fragmentation mechanics has shown that kinematic parameters are accompanied by epistemic uncertainty. The range of the fragments in the explosion of the tank has a Weibull distribution with an average value of 638 m. It is not justified to assume the initial launch angle with a uniform distribution, since its direction is defined by the shape of the fragment. The presented methodology is generally applicable to fragmentation problems in the process industry.

**Keywords:** Simulation, fragmentation, explosion, cylindrical tank, risk assessment

## 1. Introduction

The most common accidents with dangerous substances involve leaks, fires and explosions [1]. If these events are an integral part of the accident chain, then they are manifested through a domino effect [2, 3]. The main reason for fires in process plants is the presence of flammable vapors [4]. Fires lead to heating of process installations and increase of pressure in them creating conditions for explosions due to BLEVE effect [5]. Explosions of process equipment due to the domino effect imply a pronounced fragmentation effect [6]. Fragmentation action in the accident chain (domino effect) is characterized by the fact that it is both a cause and a consequence of explosions [7]. The fragmentation effect during the explosion of the tank is accompanied by a very pronounced uncertainty of geometric and kinematic parameters of the fragments [8]. Large-scale accidents that have occurred in recent times are the result of progressive technological developments, and the typical examples are Toulouse [9] and Neyshabur [10]. Fragmentation barriers are used as a form of protection against the fragmentation effect [11, 12]. The fragmentation effect and the mechanism of formation during the explosion of the tank are presented in [13]. The literature recognizes the basic geometric characteristics as the number and shape of fragments, and defines the kinematic parameters through

the trajectory and velocity of the fragments [14]. An initial procedure for estimating the number and mass of a fragment of a LPG storage tank was proposed by Baker et al. [15]. This research served as a starting point for some recent studies in the field of tank fragmentation [16, 17]. Tank fragmentation analysis should identify potential hazards and risks in terms of protecting process equipment from accident escalation [18]. Fragmentation barriers are used as protection against the fragmentation effect and were originally used in nuclear plants [19]. There are several models in the literature according to which the impact energy of a fragment into the target zone is estimated based on the fragment velocity [20–22]. Accident data show that two or three fragments are usually formed during tank fragmentation [23]. It has been determined that the distinct presence of fire during the fragmentation of the tank usually gives one fragment [24]. Previous research for the number of generated fragments estimation has exclusively used the maximum entropy model [25]. This model is based on accident data and shows that explosions with more than five generated fragments are very rare accidents [26, 27].

Tank explosions with the BLEVE effect very rarely provide more than three generated fragments [28]. The implementation of the maximum entropy model is possible only if there are available accident data for this type of process equipment [29]. Fragmentation mechanics analyzes the flight of a fragment and for that purpose the literature sources state a simplified mathematical model [30]. This model is represented in all recent research and was originally proposed by Mannan [31]. Greater mass of the fragment corresponded to the higher initial kinetic energy or the initial velocity [32]. Risk assessment due to the action of fragments is very often estimated in the literature on the basis of kinetic energy of fragments [33]. This energy is usually defined by the percentage share of expansion energy [34]. Some recommendations suggest that this percentage ranges between 5% and 20% [35]. This procedure of determining the initial velocities of the fragments has significant deviations from the real values, so it can only be used for general estimation. The aerodynamic properties of the fragments have a great influence on its kinematic parameters and are reflected in the uncertainty of the shape [36]. Djelosevic and Tepic conducted a complex study of cylindrical tank fragmentation in terms of identifying aleatoric and epistemic uncertainty [37, 38]. The same authors established a correlation of geometric and kinematic parameters of fragments, stating the importance of simulation technique in fragmentation analysis. This chapter will present a general methodological framework for the study of tank fragmentation under the conditions of the BLEVE effect, which is characteristic of the gas industry [39]. The focus of this research is on the analysis of types of uncertainty that follow fragmentation parameters with special reference to fracture probabilities and elimination of conditions that introduce influential fragment sizes into the zone of epistemic uncertainty [40].

## **2. Fragmentation methodology**

Tank fragmentation implies physical separation of fragments from the tank construction itself. The basic feature of fragments is the kinetic energy they have just before hitting a target. Greater kinetic energy of the impact creates greater potential hazard as a result of the fragmentation effect of the explosion. Assessing the kinetic energy of fragments is a complex task which requires identification of geometric and kinematic parameters. The basic geometric parameters are the shape and mass of fragments, whereas the most important kinematic parameter is the initial velocity of a fragment. Geometric and kinematic parameters are not independent since the shape of a fragment affects its initial velocity and initial launch direction. Literature

resources on the assessment of geometric and kinematic parameters of fragments are scarce. Therefore, the assessment of these parameters in this paper was conducted using probabilistic and simulation techniques. The probabilistic approach will first be presented and thereafter the simulation analysis of fragmentation.

2.1 Probabilistic approach

The probabilistic approach is used for the assessment of fragment shapes, number of generated fragments as well as for the identification of aleatoric and epistemic uncertainty. The effect of uncertainty in assessing geometric and kinematic parameters is extremely important because if a parameter has the same or approximately the same probability with the change of influential factors, then it is definitely accompanied by aleatoric uncertainty. Aleatoric uncertainty is typical of those parameters whose uncertainty cannot be eliminated. On the other hand, there is epistemic uncertainty. If a parameter has epistemic uncertainty, that kind of uncertainty can be eliminated by additional research procedures and the parameter can be subjected to deterministic principles. A typical example of epistemic uncertainty is the initial launch angle of a fragment. Literature resources show that any angle value has the same probability of occurrence and thus this parameter is introduced into the zone of aleatoric uncertainty. We will show that this is not justified and that the initial launch angle of a fragment is defined by the shape of the fragment, i.e. by potential fracture lines of a tank.

Probabilistic analysis of influential fragmentation factors is an efficient way of distinguishing between epistemic and aleatoric uncertainty. The probabilistic approach is based on the use of the probabilistic mass method which was originally developed by Djelosevic and Tepic [37, 38]. The main purpose of this method is the assessment of tank fragmentation probabilities on the basis of ideal values and the mass factor. Ideal fragmentation probabilities are assessed using statistical simulation on a sufficient number of samples. The precondition for a sufficient number of statistical samples is clear convergence of results, which, in this case, is achieved with more than 100,000 samples. Ideal fragmentation probabilities were obtained under the assumption of uniform stress state and strength (homogeneity) of the material. Ideal fragmentation probabilities are those that correspond to the explosion of a tank with a uniform stress state, and the values that refer to the specific number of generated fragments are presented in **Table 1**.

Since the actual stress state of a tank is not uniform, the ideal fragmentation probabilities have to be corrected. The correction factor used is the so-called mass factor ( $f_{mass}$ ) which represents the ratio between the mass of the part of the tank with the non-uniform stress state and the total mass of the tank. Mass factor values for typical cylindrical tanks with torispherical end caps range between 0.55 and 0.75. Greater values indicate greater uniformity of the stress state and vice versa. The effect of fire contributes to greater non-uniformity so the mass factor in this case has lower values. The assessment of mass factors requires division of the tank into segments. Cylindrical tanks should be divided into three segments irrespective of their construction type and size. The first segment comprises the cylindrical part between the supports and it is defined by length  $L$  (S1) according to **Figure 1**. The other two segments (S2 and S3) comprise the parts of the tank outside the supports

Number of fragments	1	2	3	4	5	6	$\geq 7$
The probability of ideal fragmentation	1/2	1/3	1/8	1/30	1/150	1/800	5/12000

**Table 1.**  
*Ideal tank fragmentation probabilities.*



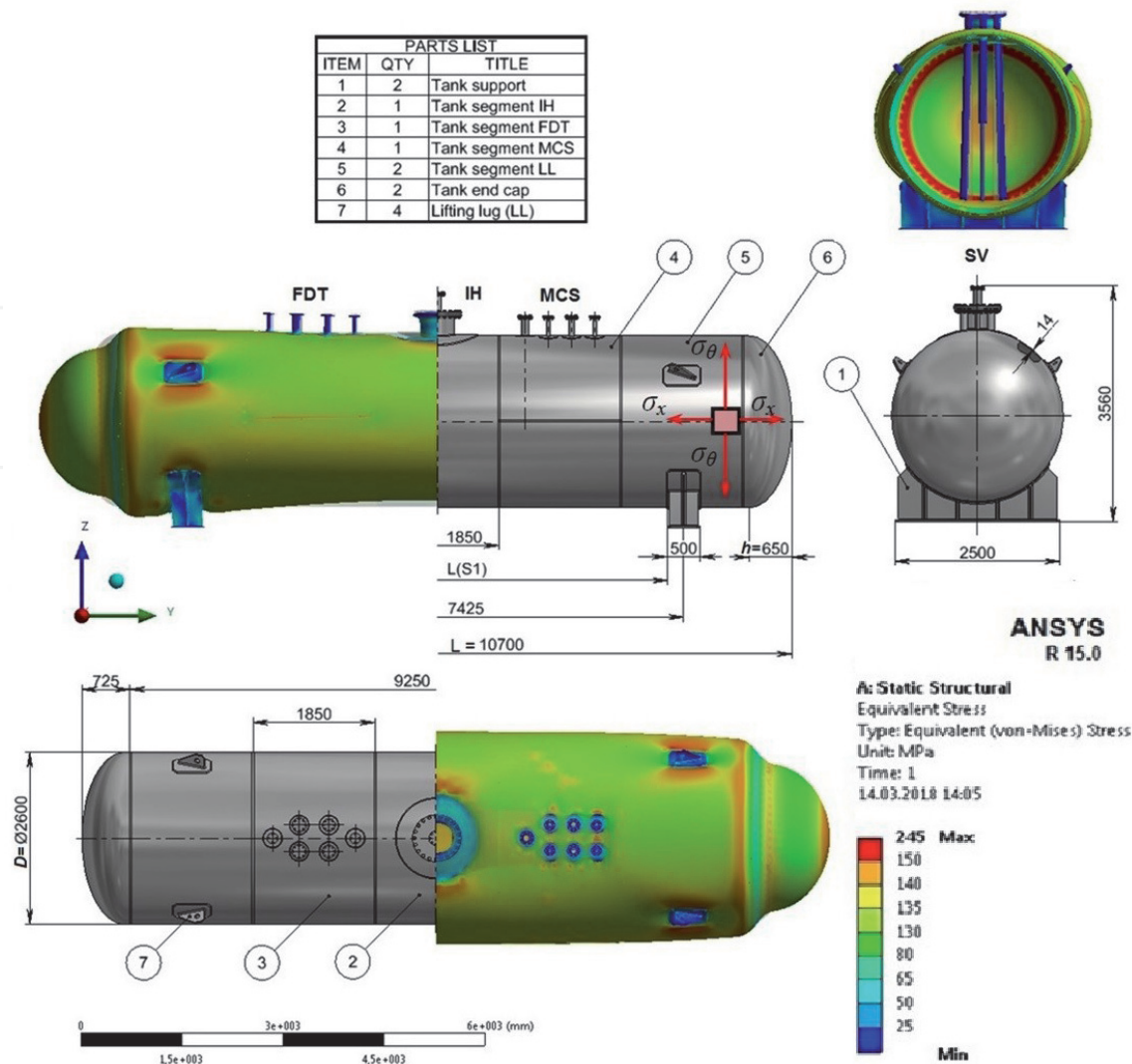


**Figure 1.**  
*Type of the tank and critical stress zones.*

and their lengths amount to  $[L - L(S1)]/2$ . Tank fracture can occur in individual segments (either S1 or S2 or S3) or in at least two segments (S1 and S2 or S1 and S3 or S2 and S3) or in all three segments (S1 and S2 and S3). Depending on the mentioned scenarios, fracture probabilities and conditional fracture probabilities resulting from tank fragmentation are derived. Fracture probabilities are associated with tank fragmentation within only one segment (either S1 or S2 or S3). Conditional fracture probabilities comprise fragments which were generated from at least two segments.

Fracture probabilities and conditional fracture probabilities according to the number of fragments are given in **Table 2**.

Conditional fracture probabilities for individual fragmentation scenarios (Sc1 ... Sc8) were obtained on the basis of fracture probabilities values for segments S1, S2 and S3. This way the probabilistic mass method enabled easy assessment of fracture probabilities according to the number of generated fragments. The literature on the subject usually mentions the entropic model for this purpose where deviation of about 50% for the probability of the third fragment is observed. The entropic model is based on accident data fitting, whereas the probabilistic mass method is independent of accident data. A comparative analysis of fracture probabilities according to the number of generated fragments for the entropic model, the probabilistic mass method and accident data is presented in **Figure 2**.

Fragment number	Fracture probability for segments [%]			Conditional probability of fracture S1 if there is damage to segments S2 and/or S3 [%]							
	S1	S2	S3	Sc1	Sc2	Sc3	Sc4	Sc5	Sc6	Sc7	Sc8
ONE (1)	35.500	6.250	6.250	32.959	2.197	2.197	0.146	54.932	3.662	3.662	0.244
	27.500	11.250	11.250	21.661	2.746	2.746	0.348	57.105	7.239	7.239	0.918
TWO (2)	25.000	4.167	4.167	22.960	0.998	0.998	0.043	68.880	2.995	2.995	0.130
	18.333	7.500	7.500	15.686	1.272	1.272	0.103	69.876	5.666	5.666	0.459
THREE (3)	9.375	1.563	1.563	9.084	0.144	0.144	0.002	87.815	1.394	1.394	0.022
	6.875	2.813	2.813	6.494	0.188	0.188	0.005	87.960	2.545	2.545	0.074
FOUR (4)	2.500	0.417	0.417	2.479	0.010	0.010	0.000	96.689	0.405	0.405	0.002
	1.833	0.750	0.750	1.806	0.014	0.014	0.000	96.700	0.731	0.731	0.006
FIVE (5)	0.500	0.083	0.083	0.499	0.000	0.000	0.000	99.334	0.083	0.083	0.000
	0.367	0.150	0.150	0.366	0.001	0.001	0.000	99.335	0.149	0.149	0.000
SIX (6)	0.094	0.016	0.016	0.094	0.000	0.000	0.000	99.875	0.016	0.016	0.000
	0.069	0.028	0.028	0.069	0.000	0.000	0.000	99.875	0.028	0.028	0.000
SEVEN (7)	0.013	0.002	0.002	0.012	0.000	0.000	0.000	99.983	0.002	0.002	0.000
	0.009	0.004	0.004	0.009	0.000	0.000	0.000	99.983	0.004	0.004	0.000
≥ EIGHT (8)	0.019	0.003	0.003	0.019	0.000	0.000	0.000	99.975	0.003	0.003	0.000
	0.014	0.006	0.006	0.014	0.000	0.000	0.000	99.975	0.006	0.006	0.000

Table 2.  
Fracture probabilities and conditional fracture probabilities of tank fragmentation.

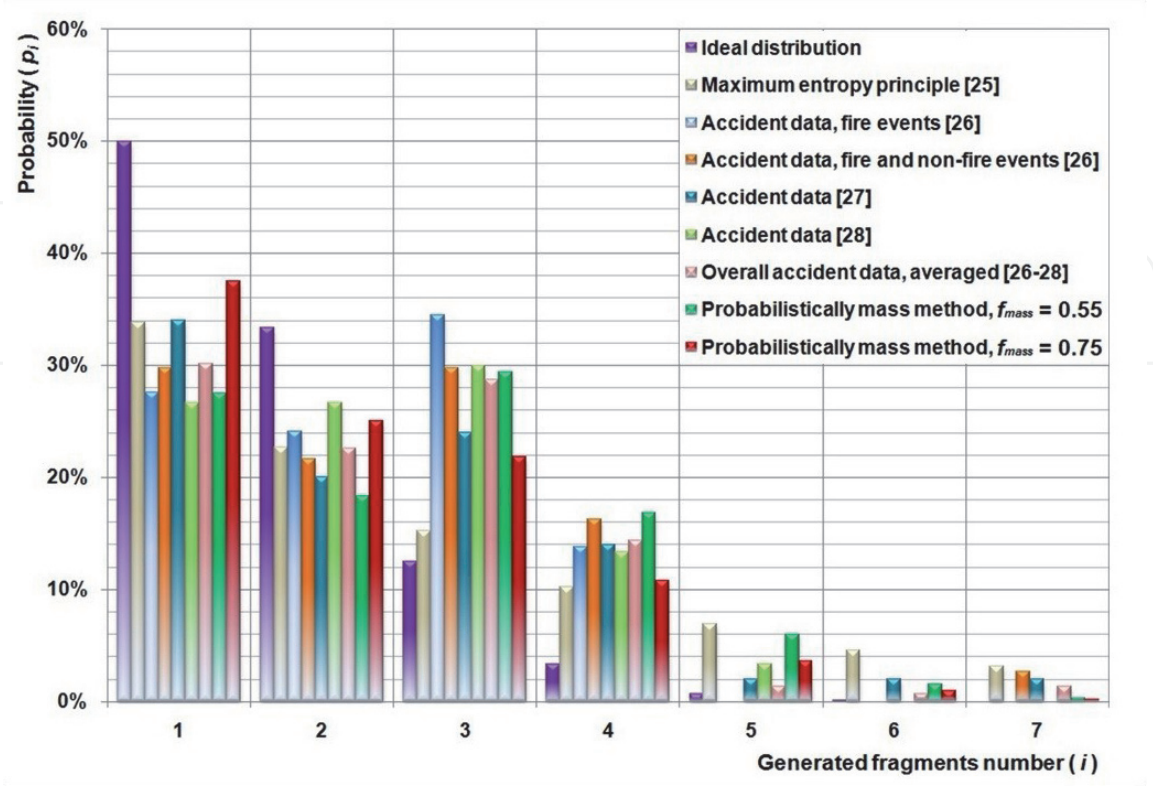


Figure 2.  
Comparative analysis of fracture probabilities.

2.2 Fracture scenarios

Fracture scenarios of fragmentation in tank explosions imply a qualitative and quantitative analysis which is performed using Failure Tree Analysis (FTA). The triggering event that leads to tank fragmentation is reaching the critical pressure. The major central events are fractures of segments 1, 2 and 3. Qualitative analysis offers eight potential scenarios (Sc1 ... Sc8). All the scenarios imply tank fragmentation apart from scenario Sc5 which excludes the possibility of tank fracture when the critical pressure is reached. Quantitative analysis implies the assessment of fracture probabilities and conditional fracture probabilities. These probabilities were assessed by means of Monte Carlo simulation using the probabilistic mass method, and they are presented in **Table 2**.

A significant part of this research deals with the assessment of the mass of fragments generated during tank explosion. For that purpose, the mass of fragments is expressed via the percent share of the empty tank mass which amounts to 12.3 t. Simulation results with over 100,000 samples show that fragments whose sum of masses ranges between 10% and 20% of the empty tank have the greatest generation probability. In this concrete case, the mass of fragments is between 1,230 kg and 2,460 kg. The maximum fragmentation probability is observed when two fragments are generated in an explosion and it amounts to around 17%.

Generation of fragments with small mass (smaller than 1% of the total mass of the tank) and generation of more than six fragments are extremely rare. The distribution of probabilities for the generated fragments depending on their mass is presented in **Figure 3**.

The probabilities of generation of only one fragment for different masses have uniform distribution, which points to aleatoric uncertainty. This means that the shape and mass of only one fragment generated in an explosion cannot be predicted

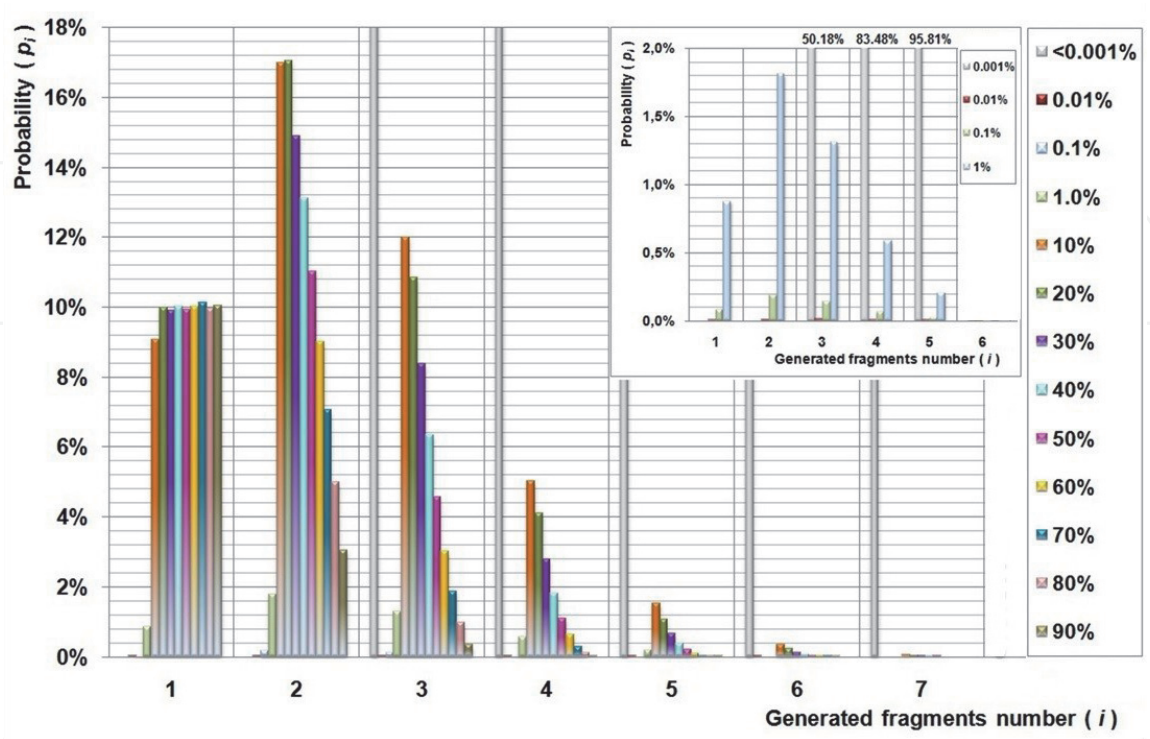


**Figure 3.**  
*Distribution of probabilities for fragments with different mass.*



with certainty. On the other hand, generation of two or more fragments is accompanied by epistemic uncertainty. This means that with adequately used methodology, the mass and shape of two or more generated fragments can be predicted with certainty with the probabilities shown in **Figure 3**.

2.3 The assessment of shape and mass of fragments

The assessment of mass and shapes of fragments requires defining fracture lines, i.e. the lines along which tank fracture occurs. Fracture lines are zones of pronounced stress of the material and are the result of different construction conditions. Definition of fracture lines implies prior pressure analysis. In this case, the analysis was performed using the ANSYS software for the operating pressure of 16.7 bar. Fracture lines can spread in those zones whose pressure exceeds 130 MPa.

Accordingly, the investigated cylindrical tank has a total of 13 typical areas from which tank fragments can be generated (**Figure 4**). The most pronounced stress of the tank is on the transition from the cylinder to the end caps of the tank. This is the reason why during an explosion a fragment containing a larger or smaller part of the end cap is almost always generated.

Tank fragmentation is most often accompanied by generation of one, two or sometimes three fragments. Their typical shapes, mass, fracture zones and generation probabilities are given in **Table 3**. The most probable scenario in tank explosion is the one with the generation of two fragments with the sum of masses of around 1,200 kg or 2,255 kg.

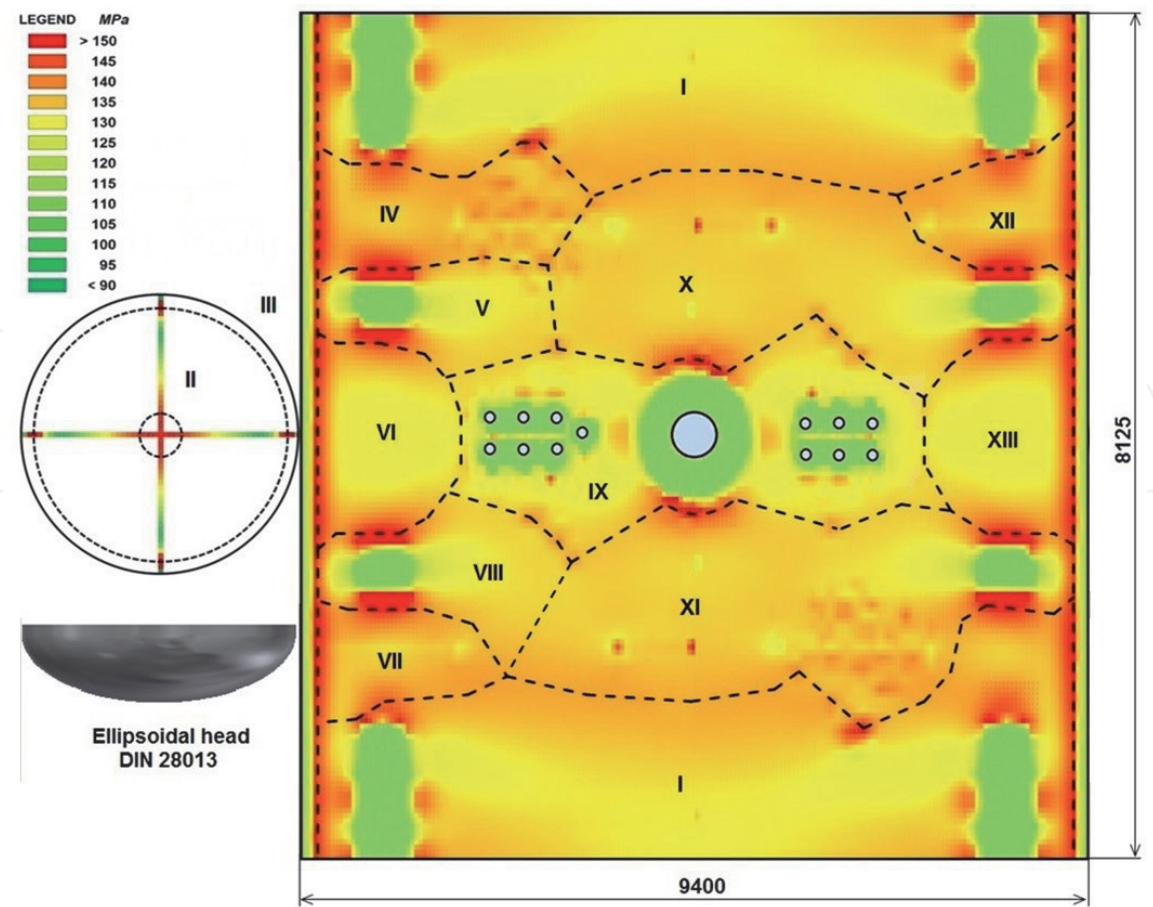
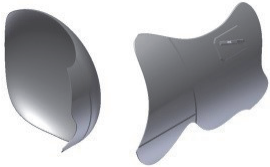




Figure 4.  
Stress state of the tank with fracture lines.



Number of fragments	Fragmentation configuration Shapes of fragments	Fragment mass [kg]	Fragmentation probability [%]	Fracture zone
2		820 480	17.04	II + III IV + V
2		205 2050	17.06	VII + VIII II + III + IV + V + VI
3		190 805 235	12.00	VII II + III V

**Table 3.**  
*Characteristic fragmentation forms of the tank.*

**3. Fragmentation mechanics**

Fragmentation mechanics involves modeling the flight of fragments created by a tank explosion. The basic characteristics of the fragments include geometric and kinematic parameters. We identified the geometric parameters in Section 2 of this chapter and they include number, mass and shape of the generated fragments. The main kinematic parameters include the initial velocity and the initial direction of the fragment launch. The literature does not provide information on the distribution of the range of fragments.

Therefore, it is not justified to assume that the range of the fragments is accompanied by a random distribution. Also, it is not justified to introduce assumptions about the uniformity of kinematic parameters of the fragments, just because we do not have enough available information about their behavior. Assuming a uniform distribution for some of the kinematic parameters, we enter an area of aleatoric uncertainty that does not allow an adequate assessment of fragmentation risk. The authors of this chapter start from the assumption that the generation of fragments does not follow a stochastic process, thus putting epistemic uncertainty in the foreground.

**3.1 Fragment flight model**

The flight of the fragment takes place under the influence of inertial, gravitational and aerodynamic forces (air resistance and lift force). The trajectory of the fragment uniquely determines the vector form of the equation of motion:

$$m_{fr} \cdot \vec{a}_{fr} = \vec{W}_D + \vec{W}_L + \vec{G} \tag{1}$$

The air resistance force ( $W_D$ ) and the thrust force ( $W_L$ ) are defined by:

$$\vec{W}_D = -\left(\frac{1}{2}\rho_v C_D A_D v_{fr}\right) \cdot \vec{v}_{fr} \tag{2}$$

$$\vec{W}_L = -\left(\frac{1}{2}\rho_v C_L A_L v_{fr}\right) \cdot \vec{v}_{fr} \tag{3}$$

The flight of each of the fragments should be observed in the local coordinate system Oxyz and then the projections of the vector differential Eq. (1) read:

$$a_{x,fr} = \dot{v}_{x,fr} = (-k_D v_{x,fr} - k_L v_{z,fr}) \sqrt{v_{x,fr}^2 + v_{z,fr}^2} \tag{4}$$

$$a_{y,fr} = \dot{v}_{y,fr} = 0 \tag{5}$$

$$a_{z,fr} = \dot{v}_{z,fr} = (k_L v_{x,fr} - k_D v_{z,fr}) \sqrt{v_{x,fr}^2 + v_{z,fr}^2} - g \tag{6}$$

Practically, the flight of the fragment is completely described by (4), (5) and (6), since there is no motion in the direction of the y-axis (that is why we observed the motion in the local coordinate system). The Taylor’s series method was used to solve the coupled system of nonlinear differential equations. The ratio of the velocity components initially defines the initial launch angle of the fragment (Figure 5). This simply proves that the initial launch angle is not accompanied by a stochastic distribution.

3.2 Initial conditions

The initial conditions define the kinematic parameters at the initial moment (at the moment of the tank explosion). These conditions are necessary for initiating the procedure of numerical solution of differential equations and read:

$$x_{fr}(t_0) = x_0 \wedge z_{fr}(t_0) = z_0 \tag{7}$$

$$v_{x,fr}(t_0) = v_{x_0} \wedge v_{z,fr}(t_0) = v_{z_0} \tag{8}$$

$$\dot{v}_{x,fr}(t_0) = a_{x_0} \wedge \dot{v}_{z,fr}(t_0) = a_{z_0} \tag{9}$$

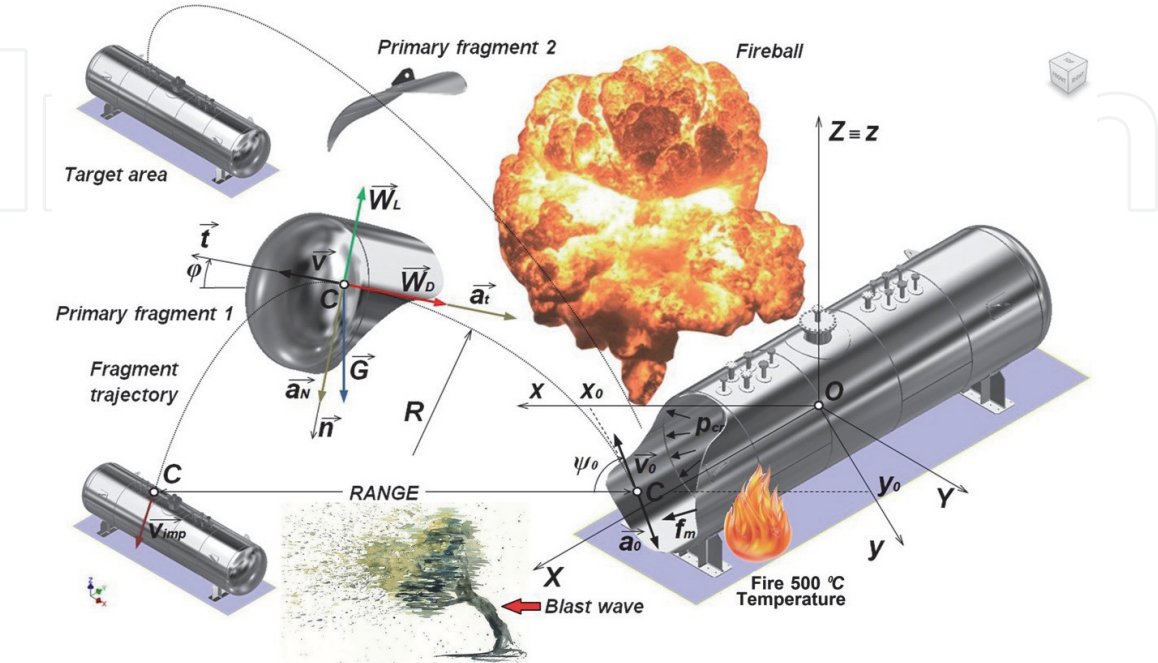


Figure 5.  
Kinematic parameters due to tank fragmentation.

These values are used as the first step in the numerical procedure and they are of unknown magnitude at the moment. At this level we know that the initial velocity is not independent of the initial acceleration of the fragments. The components of velocity at any moment  $t$  read as follows:

$$v_{x,fr} = \sqrt{\frac{(-a_x)}{k_D + k_L \cdot tg\phi}} \cdot \frac{1}{\sqrt[4]{1 + tg^2\phi}} \quad (10)$$

$$v_{z,fr} = \sqrt{\frac{(-a_z)}{k_D + k_L \cdot tg\phi}} \cdot \frac{tg\phi}{\sqrt[4]{1 + tg^2\phi}} \quad (11)$$

The direction of the fragment velocity can be determined at any time during the flight of the fragment, including the initial moment using the expression:

$$\phi = arctg\left(\frac{v_{z,fr}}{v_{x,fr}}\right) = arctg\left[\frac{\left(\frac{k_L}{k_D}\right) \cdot (-a_x) + (-a_z) - g}{(-a_x) + \left(\frac{k_L}{k_D}\right) \cdot a_z + g}\right] \quad (12)$$

In order to obtain the initial launch angle of a fragment, it is necessary to know the components of the initial acceleration. In the continuation of this chapter, we show how the initial acceleration occurs. It is important to point out that (12) shows an unjustified assumption about the uniformity of the initial acceleration. Thus, the initial launch angle as a kinematic parameter is classified in the category of epistemic uncertainty. Literature sources in this area do not use the initial acceleration parameter, although it is a way to remove uncertainty regarding a reliable fragmentation risk assessment.

### 3.3 Defining the initial acceleration

We have previously come to the conclusion that in order to define the initial velocity and the initial launch angle of a fragment, it is necessary to know the initial acceleration. Hence the idea and justification for introducing this kinematic parameter into fragmentation analysis. The initial acceleration is proportional to the force of pressure on the fragment. This force is created by the critical pressure  $p_{cr}$  acting on the inner surface of the fragment. The proportion of explosive energy transferred to the fragment is limited by the action of critical pressure. This means that the proportion of explosive energy of the fragment transferred to the fragment depends on the tensile strength of the material.

The procedure for determining the initial acceleration is based on this assumption. The lower tensile strength gives less initial kinetic energy of the fragment. Fragment generation occurs when the von Mises's stress reaches a critical value under the action of internal tank pressure and is defined as:

$$\sigma_{cr} = \sqrt{\sigma_x^2 + \sigma_\theta^2 - \sigma_x \sigma_\theta + \frac{3}{2}(\sigma_x - \sigma_\theta)^2} = 102 \cdot p_{cr} \quad (13)$$

Where the corresponding components of the von Mises's stress are given by:

$$\begin{aligned} \sigma_x &= 101 \cdot p_{cr} \\ \sigma_\theta &= 105 \cdot p_{cr} \end{aligned} \quad (14)$$

Separation of fragments from the tank as a whole occurs when the critical stress reaches the value of tensile strength of the material  $f_m$ , so the critical pressure is determined as  $p_{cr} = f_m/102$ . Accordingly, the initial acceleration of a fragment can be defined by:

$$a_o = \frac{F}{m_{fr}} = \frac{p_{cr} A_{fr}}{\rho \delta A_{fr}} = \frac{f_m}{102 \rho \delta} = const \tag{15}$$

This proves that the initial acceleration has a constant value for a certain type of steel from which the tank is made. LPG transport and storage tanks have a constant wall thickness of 14 mm. The density of steel  $\rho$  is also constant and amounts to 7850 kg/m<sup>3</sup>.

Thus, by knowing the initial acceleration, we are able to define the initial velocity and the initial launch angle, as well as all other kinematic parameters at any time during the flight of the fragment. It should be borne in mind that the initial acceleration depends on the tensile strength of the material whose values are subject to variation with temperature changes. The change in the influence values on the range of the fragment is given in **Table 4**.

3.4 Fragments range

Based on a mathematical model that describes the flight of the fragment and the initial acceleration, we are able to determine the range of the fragments. For this purpose, all geometric and kinematic parameters will be classified into two groups. The first group consists of invariant parameters and their value is fixed. The second group consists of variable parameters, ie those whose value changes during the flight of the fragment. This group includes the coefficients of aerodynamic and thrust acceleration  $k_L$  and  $k_D$ . The invariant parameters are fully defined and their value is not subject to variation during the flight of the fragment (tank wall thickness, tensile strength and specific weight of the material). Variable parameters change during the flight of the fragment due to the rotation of the fragment or some other effects. Variable parameters are defined via the air resistance coefficient  $C_D$  and the thrust coefficient  $C_L$ .

The literature gives approximate values of these coefficients which depend on the shape of the fragment. Smaller fragments whose mass does not exceed a few hundred kilograms generally have the shape of a shell (shells are aerodynamic shapes), so they have a pronounced thrust effect. In order to estimate the range of the fragments, the fluctuation of variable parameters is performed, whereby different trajectories of the fragments are obtained. These trajectories enable the definition of the limit values of the coefficients  $k_L$  and  $k_D$ . Parabolic trajectories of

Parameter	Temperature [°C]						
	20	200	400	500	600	800	900
Tensile strength $R_m$ [MPa]	500	469	373	252	117	23	11
Critical pressure $p_{cr}$ [bar]	48.5	45.5	36.2	24.5	11.4	2.2	1.1
Initial acceleration $a_o$ [m/s <sup>2</sup> ]	43,746	41,034	32,635	22,048	10,237	2,012	962
Initial velocity $v_o$ [m/s]	1,985	1,923	1,715	1,409	960	426	294
Average range $R_{avg}$ [m]	395.6	394.3	389.3	380.0	359.1	303.1	272.2

**Table 4.**  
*Temperature influence on the influence values of the fragment range.*



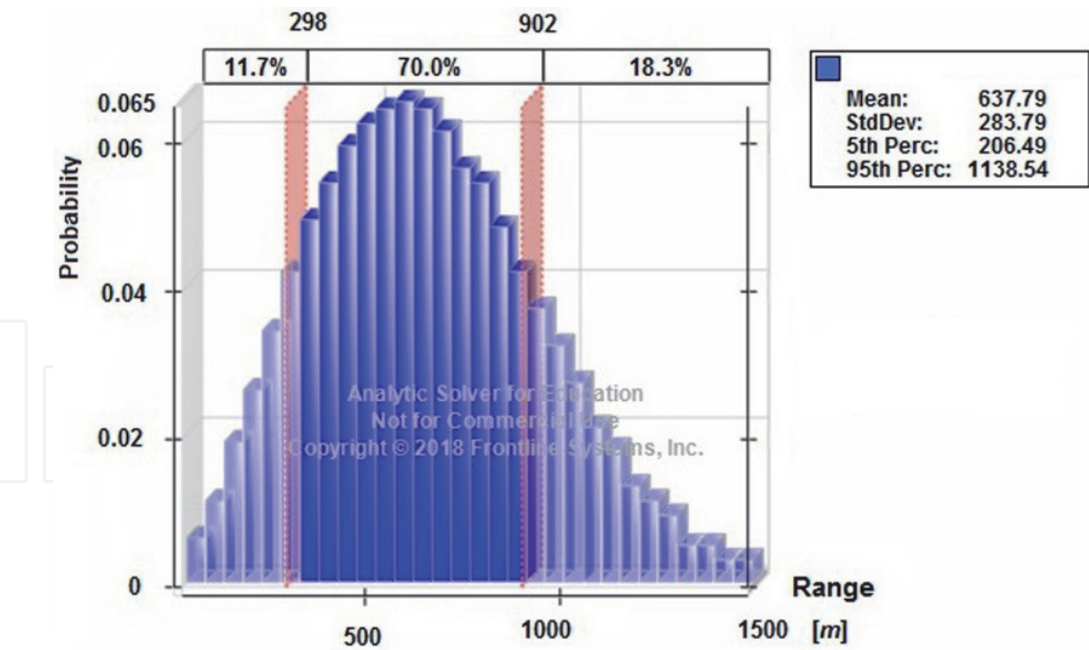


**Figure 6.**  
*Distribution of the range of typical shaped fragments.*

small height (fragment reaches small range and small height) as well as pointed trajectories (fragments reach large height and relatively small range) are very rare and represent boundary cases for the selection of coefficients  $k_L$  and  $k_D$ .

Fragment range estimation was realized by Monte Carlo simulation by processing 240 different samples for different fragmentation parameters. Fragments of up to a few hundred kilograms launched at an angle of up to  $35^\circ$  can be adequately represented by the Weibull's distribution with parameters 2.3 and 723.8 as shown in **Figure 6**.

The maximum probability of 6.5% corresponds to fragments with a range between 613 m and 663 m. This means that 6.5% of the total number of generated fragments will fall to the target between these distances.

#### 4. Fragmentation simulation model

The basic questions that are asked in the simulation model of fragmentation are related to the assessment of fragmentation density and sector angle. Fragmentation density refers to the number of fragments whose range will correspond to an area. The sector angle refers to the most common angle in the horizontal plane at which the fragments will burst due to the explosion of the tank. The simulation model of fragmentation is based on the research given in Sections 2 and 3.

##### 4.1 Assessment of fragmentation density

The density of fragments is estimated based on the results of fragmentation mechanics for different trajectories, masses and shapes of fragments. Assessment of fragment density requires the definition of appropriate distribution functions depending on the mass, the initial launch angle of the fragment and the limit values of the coefficients  $k_L$  i  $k_D$ . The considered masses of fragments are in the range from 200 kg to 200 kg, while the initial angles take values from  $5^\circ$  to  $35^\circ$ . The characteristic density functions for the defined parameters are given in **Table 5**.

Mass	Init. ang.	Coeff. of drag/lift accel. $\times 10^{-4}$ [ $m^{-1}$ ]				Type of probability density function (pdf)	Parameters of pdf	
$m_f$ [kg]	$\psi_0$ [°]	$k_{D,min}$	$k_{D,max}$	$k_{L,min}$	$k_{L,max}$		$a$	$b$
200	15	60	150	0	30	Rayleigh	264.436	—
500	15	50	80	0	22	Weibull	4.150	667.458
500	25	50	80	0	20	Gamma	10.978	51.535
800	5	40	80	0	25	Rayleigh	486.687	—
800	15	40	70	0	21	Log Normal	671.079	212.938
1350	5	39	60	0	16	Gamma	11.678	64.910
1350	15	39	60	0	15	Log Normal	802.359	228.446
1350	35	35	59	0	13	Weibull	2.984	773.223
2000	15	31	55	0	16	Weibull	2.910	890.345

**Table 5.**  
*Fragmentation densities for characteristic fragments.*

4.2 Sector angle assessment

The sector angle is the angle in the horizontal plane under which the fragment is launched. The explosion of the cylindrical tanks is accompanied by the generation of fragments from segments 1, 2 and 3 according to **Figure 1**. If the fragments belong only to segment 1, then their bursting is done exclusively in the axial direction. If the fragments belong only to segments 2 and 3, then the scattering of the fragments takes place in the action direction. In practice, the most common cases are when we have the generation of fragments from segments 1 and 2 or 1 and 3. Therefore, the first step in assessment the sector angle is to define the fragmentation probabilities by tank segments. For this purpose, the results on fracture and conditional fracture probabilities presented in Section 2 are used. Limit values of fragmentation probabilities by the number of generated fragments are given in **Table 6**.

The sector angles  $\alpha$  and  $\beta$  are determined on the basis of the following formula:

$$p_f \left( 1 - \frac{90^0 - \beta}{\alpha} \right) = \frac{11}{26} \tag{16}$$

The condition should be added to the previous formula:  $\alpha + \beta = \pi/2$ , where  $p_f$  is the fragmentation probability of the tank corresponding to the first segment (S1).

Segment	Value	Fragmentation probability ( $p_f$ ) for the number of generated fragments [%]							
		1	2	3	4	5	6	7	$\geq 8$
1   (2 and/or 3)	max	83.21	80.33	76.94	75.48	75.04	74.60	75.00	76.00
	min	64.11	60.86	57.11	55.54	55.26	55.20	52.94	53.85
Only 2 or 3	min	16.25	19.25	22.88	24.46	24.96	25.40	25.00	24.00
	max	33.75	37.62	42.28	44.28	44.74	44.80	47.06	46.15
Only 2 and 3	min	0.54	0.42	0.18	0.06	0.00	0.00	0.00	0.00
	max	2.14	1.52	0.61	0.18	0.00	0.00	0.00	0.00

**Table 6.**  
*Fragmentation probabilities by number of generated fragments.*

Sectoral angle	Value	Sectoral angle ( $2\alpha$ and $2\beta$ ) for the number of generated fragments							
		1	2	3	4	5	6	7	$\geq 8$
$2\alpha$ [°]	max	275.4	287.8	283.0	285.0	285.6	286.2	285.8	284.4
	min	303.4	310.0	318.4	322.2	323.0	323.2	329.2	326.6
$2\beta$ [°]	max	84.6	81.2	77.0	75.0	74.4	73.8	74.2	75.6
	min	56.6	50.0	41.6	37.8	37.0	36.8	30.8	33.4

Table 7.  
Sector angles by number of fragments generated.

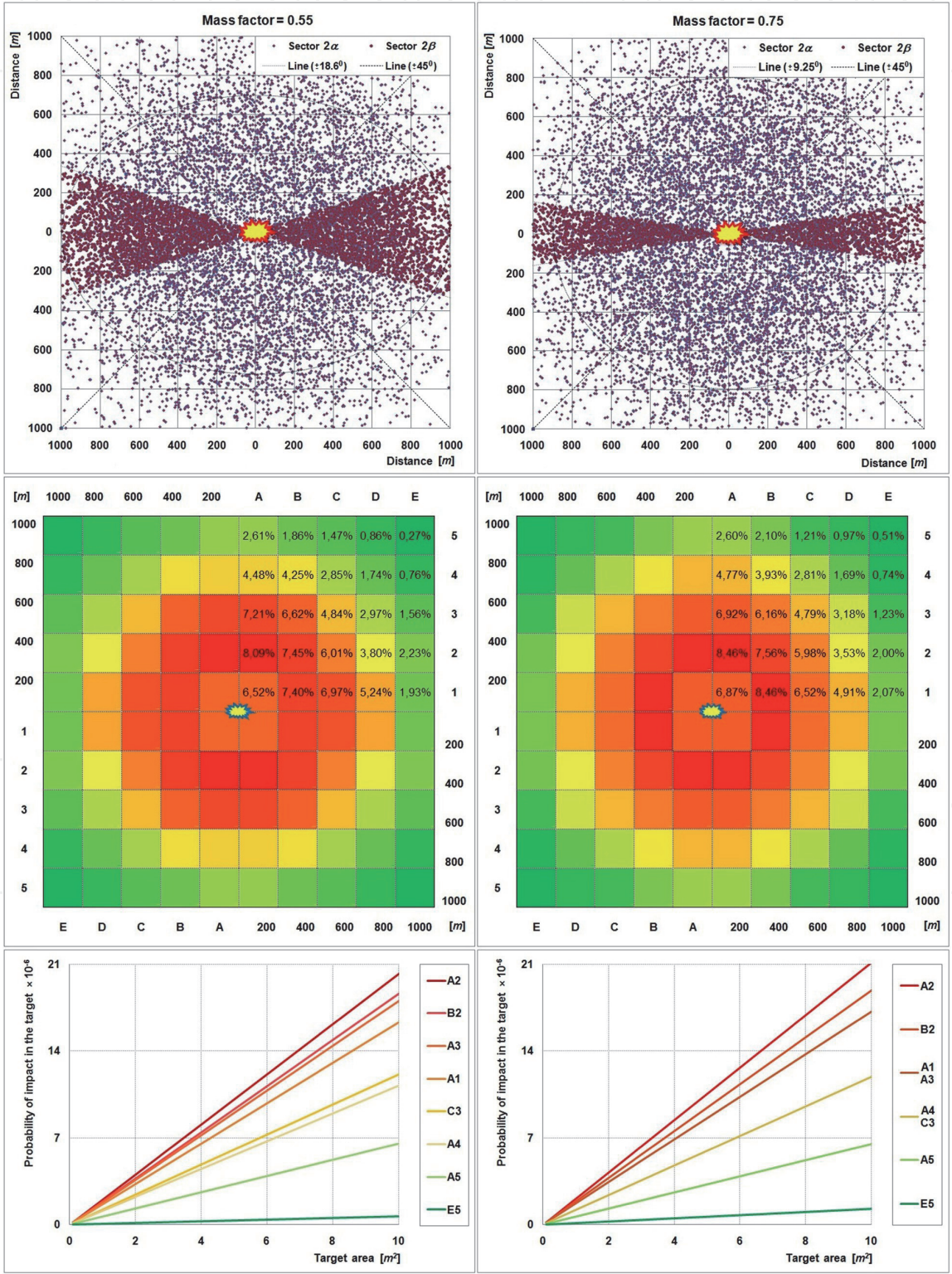


Figure 7.  
Burst simulation with risk matrix.



Sector area  $2\alpha$  covers fragmentation zones in which fragments generated predominantly from the cylindrical part of the tank are located (S1). Sector angle  $2\beta$  covers the area corresponding to the fragments generated from segments 2 and 3 (S2 i S3). Sector angles by number of generated fragments are given in **Table 7**.

## 5. Risk assessment

The risk assessment is the final phase of the fragmentation analysis due to the explosion of the LPG tank. Defining fracture probabilities, shape and mass of fragments, as well as kinematic parameters are the basis for defining fragmentation density and sector angles. The fragmentation risk assessment is performed based on the results given in Section 4. Research has shown that the fragmentation effect of a 50,000-liter tank can endanger objects and people at distances greater than 1,000 meters. Therefore, fragmentation stands out as the dominant hazard versus shock wave and thermal effect during tank explosion. Fragmentation risk assessment is carried out by dividing the area around the focus of the accident into quadrants measuring  $200 \times 200$  meters within which the number of fragments is observed.

A larger number of fragments gives a higher fragmentation risk and vice versa. The fragmentation risk analysis is given for the limit values of the mass factor (0.55 and 0.75), so we obtain the limit values of the fragmentation risk. For example, for quadrant D1 we have that the limit values of fragmentation risk are 5.24% and 4.91%, which gives an average value of 5.08%. Although there is a significant deviation between the limit values of the mass factor (0.55 and 0.75), based on the appropriate risk matrices, we can conclude that the deviation of the limit values of fragmentation risk is only a few percent. This indicates that the presented methodology based on the identification of uncertainties provides convergent and reliable solutions in the assessment of fragmentation risk. Simulations of fragment bursting as well as risk matrices are shown in **Figure 7**.

## 6. Conclusions

In this chapter, a fragmentation simulation model for risk assessment due to the explosion of a cylindrical tank is presented. According to the literature, fragmentation models exclusively use accident data. In addition, parameters for which there is insufficient information available are assumed with a uniform distribution. These are the main shortcomings of existing fragmentation models. These shortcomings have been remedied by applying the proposed fragmentation model. The simulation of fragment scattering is considered through the issue of uncertainty in the estimation of geometric and kinematic parameters. Fracture probabilities were estimated without available accident data for the considered tank type. Fragmentation mechanics enabled the definition of characteristic trajectories and the definition of limit values for coefficients  $k_L$  i  $k_D$ . Introducing the initial acceleration into the analysis, we came to know about the correlation of certain geometric and kinematic parameters of the fragment. Most of the influential parameters are accompanied by epistemic uncertainty, so the initial velocity cannot be estimated on the basis of the explosive energy of the tank, nor can the initial launch angle of the fragment be assumed by a stochastic distribution. Fragments weighing up to a few hundred kilograms are best represented by the Weibull distribution, and the most probable range of the fragments is between 670 m and 680 m. The risk matrix is given per square meter for an area of  $4 \text{ km}^2$ . The probability of impact of the fragment in the base target of  $10 \text{ m}^2$  is from  $1.6 \cdot 10^{-5}$  to  $2.1 \cdot 10^{-5}$ .



## Acknowledgements

This work has been partially supported by the Ministry of Education and Science of the Republic of Serbia within the Project No. 34014 and by the project “Naučni i pedagoški rad na doktorskim studijama”, University of Novi Sad, Faculty of Technical Sciences.

## Nomenclature


$D$	External diameter of the tank ( $D = 2600 \text{ mm}$ )
$h$	Height of the elliptic head ( $h = 650 \text{ mm}$ )
$\delta$	Wall thickness of the tank ( $\delta = 14 \text{ mm}$ )
$p$	Operating pressure of the tank ( $p = 16.7 \text{ MPa}$ )
$\sigma_x$	Longitudinal stress of the tank
$\sigma_\theta$	Circumference stress of the tank
$a_0$	Initial acceleration of the fragment
$F$	The inertial force of the fragment
$\rho$	Density of steel S355J2G3 ( $\rho = 7850 \text{ kg/m}^3$ )
$p_{cr}$	Critical tank pressure
$f_m$	Tensile strength of steel S355J2G3
$m_{fr}$	Mass of the fragment
$W_D$	Force of air resistance during flight of the fragment
$W_L$	Lifting force of the fragment
$G$	Gravitational force ( $G = m_{fr} \cdot g, g = 9,81 \text{ m/s}^2$ )
$\rho_{air}$	Air density ( $\rho_{air} = 1.20 \text{ kg/m}^3$ )
$C_D$	Coefficient of force of air resistance
$C_L$	Coefficient of lift force
$A_D$	The area of the frontal projection of the fragment
$A_L$	The area of the lateral projection of the fragment
$v_{fr}$	Velocity of the fragment
$a_{fr}$	Acceleration of the fragment
$k_D$	Coefficient of drag acceleration
$k_L$	Coefficient of lift acceleration
$x$	Horizontal coordinate
$y$	Vertical coordinate
$\Delta t$	Time interval

## Author details

Mirko Djelosevic\* and Goran Tepic  
Faculty of Technical Sciences, University of Novi Sad, Novi Sad, Serbia

\*Address all correspondence to: [djelosevic.m@uns.ac.rs](mailto:djelosevic.m@uns.ac.rs)

## IntechOpen

© 2021 The Author(s). Licensee IntechOpen. This chapter is distributed under the terms of the Creative Commons Attribution License (<http://creativecommons.org/licenses/by/3.0>), which permits unrestricted use, distribution, and reproduction in any medium, provided the original work is properly cited. 

## References

- [1] Hemmatian B, Abdolhamidzadeh B, Dabra R.M, Casal J: The significance of domino effect in chemical accidents. *J. Loss Prev. Process Ind.* 2014;29:30-38. Doi:10.1016/j.jlp.2014.01.003
- [2] Abdolhamidzadeh B, Abbasi T, Rashtchian D, Abbasi S.A: Domino effect in process industry accidents – An inventory of past events and identification of some patterns. *J. Loss Prev. Process Ind.* 2011;24:575-593. Doi: 10.1016/j.jlp.2010.06.013
- [3] Dabra R.M, Palacios A, Casal J: Domino effect in chemical accidents: Main features and accident sequences. *J. Hazard. Mater.* 2010;183:565-573. Doi: 10.1016/j.jhazmat.2010.07.061
- [4] Bariha N, Mishra I.M, Srivastava V. C. Fire and explosion hazard analysis during surface transport of liquefied petroleum gas (LPG): a case study of LPG truck tanker accident in Kannur, Kerala, India. *J. Loss Prev. Process Ind.* 2016; 40:449-460. Doi:10.1016/j.jlp.2016.01.020
- [5] Eckhoff R.K: Boiling liquid expanding vapor explosions (BLEVEs): A brief review, *J. Loss Prev. Process Ind.* 2014;32:30-43. Doi: 10.1016/j.jlp.2014.06.008
- [6] Sun D, Jiang J, Zhang M, Wang Z: Influence of the source size on domino effect risk caused by fragments. *J. Loss Prev. Process Ind.* 2015;35:211-223. Doi: 10.1016/j.jlp.2015.05.005
- [7] Khan F.I, Abbasi S.A: Major accidents in process industries and an analysis of causes and consequences. *J. Loss Prev. Process Ind.* 1999;12:361-378. Doi: 10.1016/S0950-4230(98)00062-X
- [8] Khakzad N, Amyotte P, Cozzani V, Reniers G, Pasman H. How to address model uncertainty in the escalation of domino effects? *J. Loss Prev. Process Ind.* 2018; 54:9-56. Doi:10.1016/j.jlp.2018.03.001.
- [9] Lang T, Schwoebel V, Diène E, Bauvin E, Garrigue E, Lapierre-Duval K, Guinard A, Cassadou S. Assessing post-disaster consequences for health at the population level: experience from the AZF factory explosion in Toulouse. *J Epidemiol Community Health.* 2007; 61 (2):103–107. Doi:10.1136/jech.2005.043331
- [10] Jahangiri K, Ghodsi H, Khodadadizadeh A, Yousef Nezhad S. Pattern and nature of Neyshabur train explosion blast injuries. *World J. Emerg. Surg.* 2018;13(3). Doi:10.1186/s13017-018-0164-7.
- [11] Landucci G, Argenti F, Spadoni G, Cozzani V. Domino effect frequency assessment: The role of safety barriers. *J. Loss Prev. Process Ind.* 2016;44:706-717. Doi:10.1016/j.jlp.2016.03.006
- [12] Kang J, Zhang J, Gao J. Analysis of the safety barrier function: Accidents caused by the failure of safety barriers and quantitative evaluation of their performance. *J. Loss Prev. Process Ind.* 2016; 43:361-371. Doi:10.1016/j.jlp.2016.06.010
- [13] Baker W.E, Cox P.A, Westine P.S, Kulesz J.J, Strehlow R.A. *Explosion Hazards and Evaluation*, Elsevier, Amsterdam, 1983.
- [14] CCPS, *Guidelines for Evaluating the Characteristics of Vapor Cloud Explosions, Flash Fires and BLEVE's*, Center for Chemical Process Safety, American Institute of Chemical Engineers, New York, 1994.
- [15] Baker W.E, Kulesz J.J, Ricker R.E, Bessey Westine P.S, Parr V.B. *Workbook for Predicting Pressure Wave and Fragment Effects of Exploding Propellant Tanks and Gas*

Storage Vessels. NASA CR-134906. NASA Scientific and Technical Information Office, 1997, Washington.

[16] Hauptmanns U. A Monte-Carlo based procedure for treating the flight of missiles from tank explosions. *Prob. Eng. Mech.* 2001;16:307-312. Doi: 10.1016/S0266-8920(01)00023-6

[17] Hauptmanns U. A procedure for analyzing the flight of missiles from explosions of cylindrical vessels. *J. Loss Prev. Process Ind.* 2001;21:395-402. Doi: 10.1016/S0950-4230(01)00011-0

[18] Sun D, Jiang J, Zhang M, Wang Z, Zang Y, Yan L, Zhang H, Du X, Zou Y. Investigation on the approach of intercepting fragments generated by vessel explosion using barrier net. *J. Loss Prev. Process Ind.* 2017;49:989-996.

[19] Moore C.V. The design of barricades for hazardous pressure systems. *Nucl. Eng. Des.* 1967;5:81-97. Doi:10.1016/0029-5493(67)90081-7

[20] Brode H.L. Blast wave from a spherical charge. *Phys. Fluids.* 1959; 2: 217-229. Doi:10.1063/1.1705911

[21] Baker W.E. *Explosions in Air*, University of Texas Press, Austin, 1973.

[22] Baum M.R. The velocity of missiles generated by the disintegration of gas pressurized vessels and pipes. *Trans. ASME.* 1984;106:362-368. Doi:10.1115/1.3264365

[23] Nguyen Q.B, Mébarki A.M, Saada R. A, Mercier F, Reimeringer M. Integrated probabilistic framework for domino effect and risk analysis. *J. Loss Prev. Process Ind.* 2009;40:892-901. Doi: 10.1016/j.advengsoft.2009.01.002

[24] Mishra K.B. Multiple BLEVEs and fireballs of gas bottles: Case of a Russian road carrier accident. *J. Loss Prev. Process Ind.* 2016;41:60-67. Doi: 10.1016/j.jlp.2016.03.003

[25] Mébarki A, Mercier F, Nguyen Q.B, Saada R.A. Structural fragments and explosions in industrial facilities. Part I: Probabilistic description of the source terms. *J. Loss Prev. Process Ind.* 2009;22: 408-416. Doi:10.1016/j.jlp.2009.02.006

[26] Holden P.L, Reeves A.B, Fragment hazards from failures of pressurised liquefied gas vessels. *IchemE Symposium Series No. 93.* 1985:205.

[27] Holden P.L. Assessment of missile hazards: Review of incident experience relevant to major hazard plant. *Safety Reliab. Directorate, Health Safety Directorate*, 1988.

[28] Nguyen Q.B, Mebarki A, Mercier F., Saada R.A, Reimeringer M. The domino effect and integrated probabilistic approaches for risk analysis. In: *proceedings of the Eight International Conference on Computational Structures Technology*, Sep. 2006, Las Palmas, Spain. 2006. p. 27-34. <hal-00719771>

[29] Sun D, Jiang J, Zhang M, Wang Z, Huang G, Qiao J. Parametric approach of the domino effect for structural fragments. *J. Loss Prev. Process Ind.* 2012;25:114-126. Doi:10.1016/j.jlp.2011.06.029

[30] Gubinelli G, Zanelli S, Cozzani V. A simplified model for the assessment of the impact probability of fragments. *J. Hazard. Mater.* 2016; A116:175-187. Doi: 10.1016/j.jhazmat.2004.09.002

[31] Mannan S. *Lees' Loss Prevention in the Process Industries*, fourth ed., Elsevier, Oxford, 2012.

[32] Baum M.R. The velocity of large missiles resulting from axial rupture of gas pressurised cylindrical vessels. *J. Loss Prev. Process Ind.* 2001;14:199-203. Doi:10.1016/S0950-4230(00)00039-5

[33] Mébarki A, Nguyen Q.B, Mercier F. Structural fragments and explosions in

industrial facilities. Part II: Projectile trajectory and probability of impact. J. Loss Prev. Process Ind. 2009;22:417-425. Doi:10.1016/j.jlp.2009.02.005

[34] Center for Chemical Process Safety (CCPS). Guidelines for evaluating the characteristics of vapor cloud explosions, flash fires, and BLEVEs. New York: American Institute of Chemical Engineers, 1994.

[35] Tugnoli A, Gubinelli G, Lamducci G, Cozzani V. Assessment of fragment projection hazard: Probability distributions for the initial direction of fragments. J. Hazard. Mater. 2014;279: 418-427. Doi:10.1016/j.jhazmat.2014.07.034

[36] Gubinelli G, Cozzani V. Assessment of missile hazards: Evaluation of the fragment number and drag factors. J. Hazard. Mater. 2009;161:439-449. Doi: 10.1016/j.jhazmat.2008.03.116

[37] Djelosevic M, Tepic G. Identification of fragmentation mechanism and risk analysis due to explosion of cylindrical tank. J. Hazard. Mater. 2019; 362: 17-35. Doi:10.1016/j.jhazmat.2018.09.013

[38] Djelosevic M, Tepic G. Probabilistic simulation model of fragmentation risk. J. Loss Prev. Process Ind. 2019; 60:53-75. Doi:10.1016/j.jlp.2019.04.003

[39] Manescau B, Chetehouna K, Sellami I, Nait-Said R, Zidani F. BLEVE Fireball Effects in a Gas Industry: A Numerical Modeling Applied to the Case of an Algeria Gas Industry. Fire Safety and Management Awareness, July 16th 2020: Fahmina Zafar and Anujit Ghosal, IntechOpen, Doi:10.5772/intechopen.92990.

[40] Nannapaneni S, Mahadevan S. Reliability analysis under epistemic uncertainty. Rel. Eng. & Sys. Safety. 2016;155:9-20. Doi:10.1016/j.res.2016.06.005